Proc. Natl. Acad. Sci. USA
Vol. 86, pp. 4549–4553, June 1989
Developmental Biology

Collagen fibrillogenesis *in situ:* Fibril segments are intermediates in matrix assembly

DAVID E. BIRK*, EMANUEL I. ZYCBAND, DONALD A. WINKELMANN, AND ROBERT L. TRELSTAD

Department of Pathology, Robert Wood Johnson Medical School, University of Medicine and Dentistry of New Jersey, Piscataway, NJ 08854

Communicated by Jerome Gross, March 3, 1989 (received for review November 30, 1988)

ABSTRACT **The assembly of discontinuous fibril segments and bundles was studied in 14-day chicken embryo tendons by using serial sections, transmission electron microscopy, and computer-assisted image reconstruction. Fibril segments were first found in extracytoplasmic channels, the sites of their polymerization; they also were found within fibril bundles. Single fibril segments were followed over their entire length in consecutive sections, and their lengths ranged from 7 to 15 μm. Structural differences in the ends of the fibril segments were identified, suggesting that the amino/carboxyl polarity of the fibril segment is reflected in its architecture. Our data indicate that fibril segments are precursors in collagen fibril formation, and we suggest that postdepositional fusion of fibril segments may be an important process in tendon development and growth.**

Collagen is the major protein in tissues such as tendon, cornea, bone, and skin, and at least 12 different molecular forms have been isolated from vertebrates (1, 2). Type I collagen is the most abundant and plays a major role in structure stabilization. One level of organization of type I collagen molecules is into fibrils, which are long, filamentous, quasi-crystalline aggregates whose biochemical and molecular attributes have been described in detail (3). Fibrils are organized into bundles, which are themselves organized into macroaggregates such as the nearly orthogonal layers in bone and cornea, the less regular layers in dermis, and the nearly uniaxial arrangement in tendons and ligaments.

The self-assembly of type I collagen has been studied extensively *in vitro,* and many inferences about *in situ* assembly have been drawn from these studies (4). Collagen fibril formation *in situ* is a multistep process involving intracellular as well as extracellular compartments defined by the fibroblast (5). Fibroblasts exert control over collagen fibril formation in a number of ways, including control of the stoichiometry of different matrix gene products during synthesis and subsequent packaging for secretion (5, 6), vectorial discharge of macromolecules (5–7), and formation of extracellular compartments for matrix assembly (8–12). These cellular influences are well illustrated in the developing tendon, where fibril segment polymerization occurs within deep channels in the fibroblast surface, and fibril bundle formation occurs within a more peripheral extracytoplasmic compartment defined by single or adjacent fibroblasts (11, 12). This compartmentalization of the extracellular space presumably permits the fibroblast to partition the fibril segments, fibrils, fibril bundles, macroaggregates, and the processing enzymes necessary for the postdepositional modification of the polymers.

However, these observations do not explain the mechanism whereby, long, seemingly endless collagen fibrils with mechanical integrity are assembled during development, growth, and repair. In the present study, we demonstrate that 14-day chicken embryo tendon fibroblasts produce discontinuous fibril segments that presumably fuse linearly and/or laterally to form thicker, longer fibrils. The fibril segment described here introduces another intermediate into the multistep sequence of collagen assembly.

MATERIALS AND METHODS

White Leghorn chicken embryos were incubated in a humidified atmosphere and staged as described by Hamburger and Hamilton (13). Limbs were fixed *in situ* at stage 40 (day 14) in 4% paraformaldehyde/2.5% glutaraldehyde/0.1 M sodium cacodylate, pH 7.4/8 mM $CaCl_2$ for 15 min at room temperature followed by 40 min at 4°C. After fixation, the metatarsal tendons were dissected, washed in 0.1 M cacodylate buffer (pH 7.4), and further fixed with 1% OsO_4 in cacodylate buffer (pH 7.4) for 1 hr at 4°C. The tissues were washed in buffer and then in 50% ethanol and then were stained *en bloc* with ethanolic uranyl acetate (2% uranyl acetate/50% ethanol) for 1 hr at 4°C. Dehydration was continued through a cold, graded ethanol series followed by propylene oxide. The tendons were infiltrated; embedded in a fresh mixture of Polybed 812, nadic methyl anhydride, dodecenylsuccinic anhydride, and DMP-30 (Polysciences, Warrington, PA); polymerized; and sectioned (10, 11).

Sections of tendon were cut perpendicular to the tendon axis with a Reichert Ultracut E ultramicrotome and a diamond knife. Serial sections were cut at 150 or 200 nm by using the setting on the microtome, and thickness was verified from the interference colors. There was some variation in section thickness, and because all sections were collected, the given thickness should be considered a mean value. Sections were picked up onto butvar-coated 1 × 2 mm slot grids and were stained with 2% aqueous uranyl acetate for 20 min, followed by 0.2% lead citrate in 0.1 M NaOH for 5 min. The stained sections were stabilized by the evaporation of carbon, examined, and photographed at 100 kV with a Philips 420 transmission electron microscope (10, 11).

Fibrils were followed in consecutive serial sections, and computer-generated, graphic, three-dimensional renderings were produced. Areas of interest were identified in photographic prints of >150 serial sections, and the appropriate areas in 79 consecutive sections representing ≈12 μm of tissue were digitized from the negatives by using an Optronics P1000 high-resolution microdensitometer. Consecutive images were displayed on a Lexidata LEX 90/35 high-resolution graphics device interfaced with a DEC MicroVAX II computer. The fibrils in these images were aligned by inspection and contoured based on the electron density of the fibril versus the background. The fibril contours of interest were then transferred to MOVIE.BYU (Department of Civil Engineering, Brigham Young University, Provo, UT), a graphics program used for the production of three-dimensional reconstructions.

The publication costs of this article were defrayed in part by page charge payment. This article must therefore be hereby marked "*advertisement*" in accordance with 18 U.S.C. §1734 solely to indicate this fact.

*To whom reprint requests should be addressed.

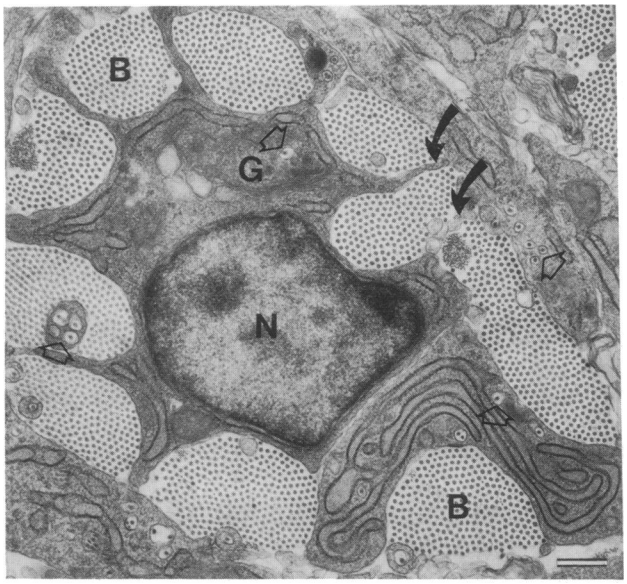

FIG. 1. Extracellular compartmentalization. This electron micrograph of a 150-nm-thick section cut perpendicular to the axis of a 14-day chicken embryo tendon shows the complexity of the fibroblast surface and the partitioning of the extracellular space into distinct domains by the fibroblast. Within these compartments, the hierarchical stages in the assembly of the matrix from fibrils to fibril bundles to macroaggregates develop. The fibril-forming channels (open arrowheads), and the bundle-forming spaces (B) are indicated. Our interpretation is that the macroaggregate-forming space is formed as cell processes retract between bundle-forming compartments (arrows) and adjacent cells, with the coalescence of bundles to form macroaggregates. N, nucleus; G, Golgi complex. (Bar = 500 nm.)

RESULTS

A hierarchy of extracytoplasmic compartments is established by the fibroblast within which three levels of matrix organization are recognized: fibril segments, fibril bundles, and macroaggregates. The complex topography of the fibroblast's surface generates this compartmentalization, and it is well illustrated in sections cut perpendicular to the axes of day 14 chicken embryo tendons (Fig. 1). At least three extracellular compartments are seen: (*i*) a series of narrow channels containing single or sometimes several (2–3) fibril segments, (*ii*) fibrils grouped as fibril bundles defined by a single fibroblast or sometimes by adjacent fibroblasts, and (*iii*) laterally associated fibril bundles, macroaggregates, defined by the apposition of two to three adjacent fibroblasts.

Fibril segments† are assembled within the first of the extracytoplasmic channels (Fig. 2). One end (termed proximal) of the fibril segments was observed within the channels, deep within the fibroblast cytoplasm, frequently in a perinuclear location. The distal end of the fibril segment is often near an operculum at the cell periphery, where the distal end of the segment terminates at or near the point where the channel opens to a bundle-forming space. Alternatively, the distal end of the segment may extend out of a channel and into a bundle for one or more micrometers before it terminates. The lengths of 25 extracytoplasmic channels were measured from serial sections without consideration of the lengths of the contained fibril segments. The channel lengths ranged from 4.7 to 17 μm, with a mean length of 9.8 ± 3.4 μm.

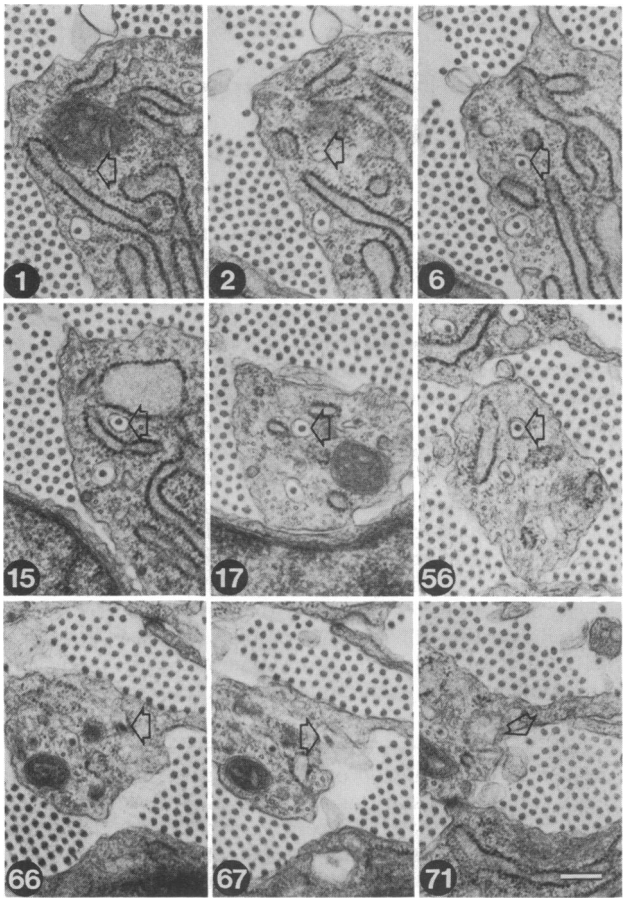

FIG. 2. Assembly and deposition of fibril segments. In this series of micrographs from serial 200-nm-thick sections, a collagen fibril, within a narrow channel (open arrowhead), is followed from its initial appearance in section 2 to its opening to the bundle-forming compartment (section 67) to its addition to a fibril bundle (section 71). The fibril-forming channels are 5–16 μm long (mean of 9.5 μm). Fibril segments assembled within these channels are seen to terminate at the opening to the extracellular space or they may enter the bundle and continue for 1 or more μm. (Bar = 250 nm.)

Fibril segments were found in extracytoplasmic channels and in fibril bundles in a manner suggesting that the fibril segment is formed in the channel and then added to a fibril bundle containing other segments of varying lengths. The length and diameters of the fibril segments in bundles were determined in serial sections. The ends of fibril segments were recognizable by their significantly smaller diameters and by their disappearance in the serial section set (Fig. 3). In Fig. 4 a single fibril segment is followed from its beginning to its termination in 55 consecutive 150-nm-thick sections. From these micrographs we calculate that this fibril segment is 7.95 μm (53 × 0.15) in length. Other fibril segments were followed in this manner, and the lengths were from 7 to 15 μm (n = 13).

The fibril segments have different rates of taper at their ends. Fig. 5 is a frequency histogram of the distance from a fibril end to a full 41-nm-diameter fibril for 50 ends. There is a clear bimodal distribution, with a peak at about 1.6 μm and a second broader peak at about 4.5 μm. There was no apparent preferred orientation of the taper within a bundle.

The serial sections of 10 neighboring fibril segments selected from Fig. 4 were reconstructed by computer-assisted techniques. This three-dimensional reconstruction is shown in Fig. 6. One fibril segment is shown in its entirety, and two

†A "fibril" is a D periodic structure of indeterminant length; a "fibril segment" is a D periodic structure of discrete length; "fibrillar elements" are fibrils and/or fibril segments; a "fibril profile" is a two-dimensional projection of a sectioned fibril or fibril segment; an "*end*" is a portion of fibril and/or fibril segment that terminates in longitudinal sections or in serial sections or is a fibril profile that is <30% of the mean fibril profile diameter.

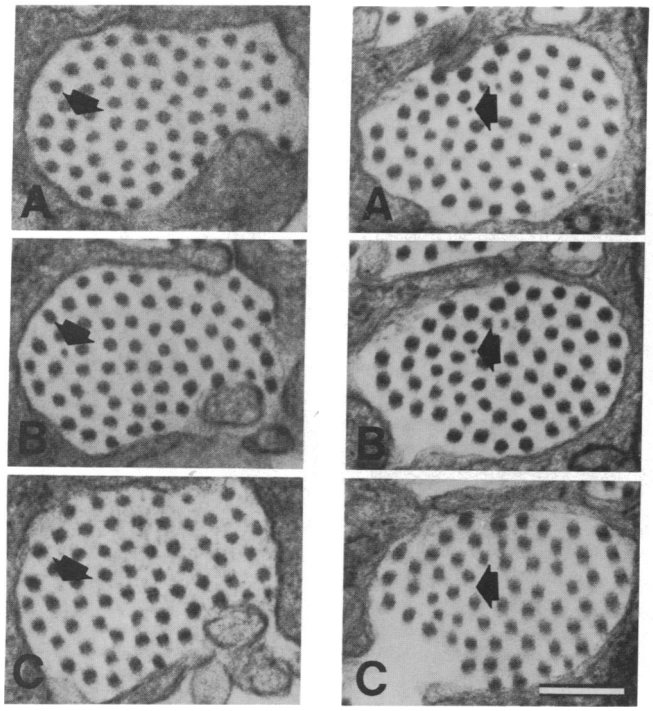

FIG. 3. Collagen fibrils are discontinuous within fibril bundles. Serial electron micrographs of 200-nm-thick sections show the ends of fibril segments within fibril bundles. Two examples of fibril ends are presented. The disappearance of two fibrils is presented. Not all plates are consecutive from *A* to *C*; however, no more than 400 nm is missing between adjacent plates. (Bar = 250 nm.)

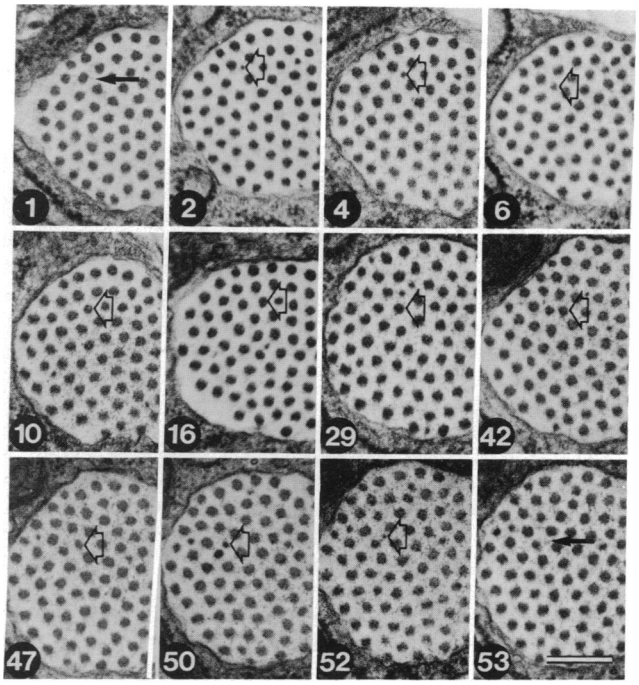

FIG. 4. Fibril segments are incorporated into fibril bundles. These serial 150-nm-thick sections are cut perpendicular to the axis of 14-day chicken embryo tendon and show both ends of a fibril segment. The ends are not present in sections 1 and 53. An end appears in section 2 and gradually reaches full diameter in section 10. The opposite end gradually disappears beginning with a full-diameter fibril in section 47 and is last seen in section 52. This corresponds to a segment length of approximately 8.0 μm. The taper of the ends is different as shown in Fig. 5. (Bar = 250 nm.)

ends of other segments also are included. This reconstruction contains data from 8.5 consecutive μm of tendon, within the entire 12.5 μm of digitized data. For the 10 fibrils followed over the 12.5-μm set, 6 had at least one end present, 1 fibril segment was totally included in the set, and 5 segments were partially included. In addition, at the limits of the reconstruction, at least 2 fibril-segment diameters narrowed, suggesting that they were approaching the ends. From these data we conclude that at least 60–80% of the fibrils in the 14-day chicken tendon are present as fibril segments. The fibril segments within this reconstruction are woven, and their spatial relationships with neighboring fibrils are constantly changing. The fibril segments were staggered with respect to one another, and no specific packing arrangement has yet been discerned other than the highly anisotropic alignment.

DISCUSSION

We present here detailed structural information on a newly recognized intermediate in collagen fibrillogenesis: the fibril segment. Fibril segments form within unique fibril-forming channels, which are extracellular compartments. The segments are then placed, deposited, or "shed" into the bundle-forming space (11, 14). The fusion of fibril segments and their addition to fibril bundles are newly recognized processes in fibril assembly. We suggest that there must be some kind of lateral and/or linear assembly to form mature, continuous fibrils during tendon development and growth.

Our data indicate that the fibril segment is a normal precursor in the formation of continuous collagen fibrils during morphogenesis. In our reconstruction of 10 fibrillar elements, at least 6–8 were present as fibril segments. Since the majority of fibrillar elements in this set are fibril segments, we assumed for the following calculation that all of the fibril profiles in cross sections at 14 days are segments and that their overlap pattern is random. Therefore, the probability (P) of finding an end if the segment has length L in a section thickness d, where $L >> d$ is: $P_{min} = 1d/L$, $P_{ave} = 1.5d/L$, and $P_{max} = 2d/L$. [If the fibril segments were not randomly arranged, we would have expected to see groups of ends in clusters. For example, if the segments were aligned with their ends in register, we would have expected to see a

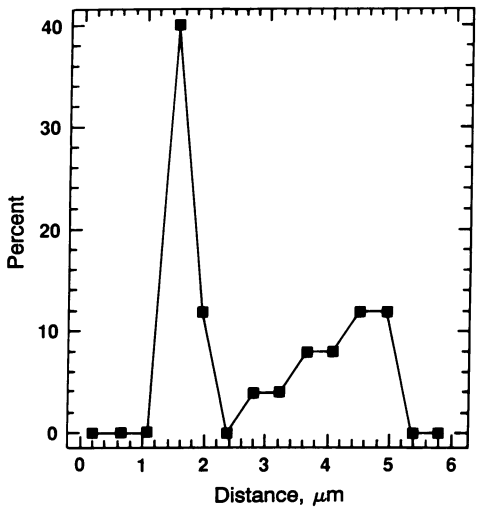

FIG. 5. Fibril segments are asymmetric. To characterize the differences seen in fibril segment ends, we measured the distance required for an end to reach full diameter. These observations were made for 50 segments in several different fibril bundles. We found that the distribution was bimodal, with a peak at about 1.6 μm and a second broader peak at about 4.5 μm. These data indicate that there may be structural differences in the amino and carboxyl termini of fibril segments. There was no apparent preferred orientation of the segments within the bundles.

large percentage of the ends in a few sections and no ends in most of the sections. Or if the segments had a regular stagger, the ends would have been clustered in sections at regular intervals. We have found the ends to be in roughly equal proportions at different levels throughout the bundle.] Our finding that ends comprise 2.9% of the fibril profiles in a 200-nm-thick section (≈1000 fibrils in 10–15 bundles were counted) indicates that the average length of the fibril seg-

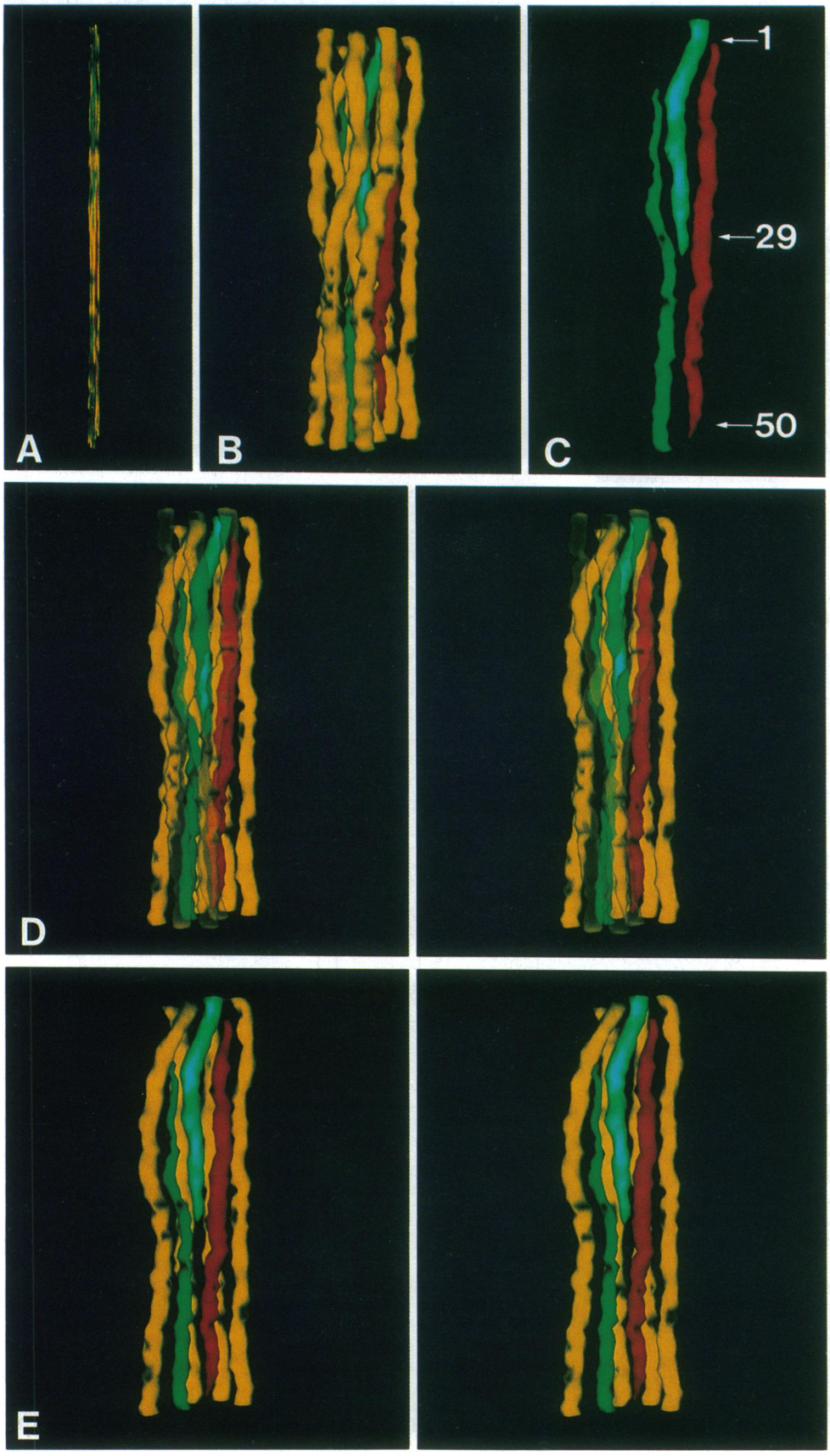

FIG. 6. Three-dimensional computer reconstruction of fibril segments. The fibril segment followed in Fig. 4 and nine surrounding fibril profiles were reconstructed for 55 consecutive 150-nm-thick sections. For presentation, not all of the fibrils seen in this group in the micrographs are present in this reconstruction; therefore, this series of fibrils appears somewhat more open than is the case in the actual bundle. The beginning and end of a fibril segment (red) are shown in relationship to other fibrils. Also shown are the termination of one neighboring fibril (cyan) and the beginning of another adjacent fibril (green) within this bundle. (*A*) Relationship of 10 different fibrils shown to scale. (*B*) Reconstruction from *A* with the *z* scale being 10% of actual. All 10 fibrils are present. In the reconstructions presented in *B–E*, this *z* scale is compressed and the same orientation is used so that the individual fibrils can be appreciated. (*C*) The three fibrils terminating within the 8.25 μm shown in this reconstuction are shown without the neighboring fibrils. Arrows indicate the level of the section numbers from Fig. 4. (*D* and *E*) Stereo pairs. In *D* the front fibrils have been made transparent, while in *E* they have been removed. It is obvious that the fibrils are discontinuous within the fibril bundles of a 14-day chicken embryo tendon and that these fibrils move in the bundle in relation to one another, with a fibril's nearest neighbors constantly changing. This produces a weaving and/or twining of the composite fibril segments.

ments (from P_{ave}) is 10.34 ± 3.45 μm, a value consistent with those determined from the serial section measurements of segments and of the extracytoplasmic channels within which they form in the fibroblast. [If all fibril ends are present in the bundle, the probability of finding an end in any section is related to $2d/L$, since a segment has two ends. Some ends are present in cell-defined channels and other bundles; therefore, the number of ends actually is between one and two. However, the number of ends also may be overestimated because of the criteria used to identify them in a single section (<30% of normal diameter).] Conversely, if we substitute the 7- to 15-μm value for segment length measured from the serial section data into the above equation, we would predict that ends would constitute between 2.0% and 4.3% of the fibril profiles in a 200-nm-thick section if all fibril profiles were segments and the segments were randomly arranged. This value is also consistent with the fibril-forming channels having a length of 9.8 μm.

The finding of a biomodal distribution for the taper of fibril segment ends suggests that the fibril segment may be asymmetric with respect to the rate of change of the diameter at the ends. However, we cannot exclude the possibility that there are two or more populations of fibril segments with differing taper rates. An asymmetric fibril segment would be consistent with work on fibril growth *in vitro*, where the amino-terminal end of the growing collagen fibril was found to decrease by four to five molecules per 67 nm, while the change at the carboxyl-terminal end was 8–10 per 67 nm (15, 16).

The identification of fibril segments as precursors in fibril formation adds another intermediate to the multistep assembly of collagen from its molecular form to the macroscopic form present in tissues. Molecular interactions driven by physiochemical forces are important during the polymerization of type I collagen molecules into fibril segments, and such interactions can be mimicked *in vitro*. What cannot be well assembled *in vitro* is a funtional, isotropic group of fibril bundles such as those found in the skin, tendon, bones, and cornea. Study of the assembly process *in situ* has indicated that the topography of the cell surface and intercellular spaces play an important role in the orientation of the discharged collagen (6–12) as well as mechanical forces (17).

For the cell to play an important role in the macroscopic assembly of the matrix, the intermediates formed by the cells must be of manageable size and shape. The factors that lead to the limitation of the lengths of the fibril segments are not known. It is conceivable that the process of assembly in the channels is simply limited by the amount of procollagen in this space. However, there might also be capping agents, analogous to those operative in other polymerizing filamentous systems, which interact with the growing segment in some complex manner to limit growth. It would appear that the fibril segment, while large, is sufficiently small to allow rearrangement by the cell. We predict that the slender cytoplasmic processes seen within bundles are "juggling" or "cradling" or "pushing" the segments into place (17, 18). Intuitively, it would seem that tension exerted by the cell on the developing matrix could more easily rearrange short segments than long segments. Moreover, the discontinuous process of fibril formation allows for angular arrangements, for intercalary growth, and even for repair. The elucidation of this segmental nature of the forming fibril offers new insight into fibril formation. The problem of fibril/cell translocation during secretion, implicit in earlier models where it was proposed that fibrils of unknown length were formed in channels (8, 10, 11), has now been resolved.

If, as we predict, there is lateral and/or linear association of fibril segments to form thicker, more continuous fibrils during maturation, then we would expect a change in fibril segment diameter and/or length with age. As yet, we have not captured this event in the micrographs from 14-day chicken embryo tendons. However, we suspect that fusion occurs both linearly and laterally, accounting for the rapid increase in fibril diameter from day 14 to day 19 of incubation (19–22). Scott (23) has already proposed that a fusion of fibrils occurs, with possible regulation via a surface coat of dermatan sulfate proteoglycan. Our data do not directly address the mechanism(s) involved in the fusion but would be consistent with the process occurring with some varying degree of overlap between adjacent segments.

During wound repair, the reweaving that occurs presumably involves the addition of segments to preexistent fibril ends. If the unique character of the "ends" persists after fusion, their exposure by proteases at the time of injury might provide a suitable old site to which newly formed segments might associate. The unusual healing properties of fetal and newborn tissues might be explained, in part, by the presence of more frequent or less modified segments (24). If rearrangements at the tissue level are more possible with short segments, then injury to a young tissue presents the cells with less difficulty in repair.

We acknowledge the assistance of Patrick Lardieri with the reconstructions. This work was supported by National Institutes of Health Grant AR37003, Research Career Development Award EY00254 to D.E.B., and an American Heart Association Established Investigator Award to D.A.W.

1. Mayne, R. & Burgeson, R. E. (1987) *Structure and Function of Collagen Types* (Academic, New York).
2. Miller, E. J. (1988) in *Collagen*, ed. Nimni, M. E. (CRC, Boca Raton, FL), Vol. 1, pp. 139–156.
3. Nimni, M. E. & Harkness, R. D. (1988) in *Collagen*, ed. Nimni, M. E. (CRC, Boca Raton, FL), Vol. 1, pp. 1–77.
4. Veis, A. & Payne, K. (1988) in *Collagen*, ed. Nimni, M. E. (CRC, Boca Raton, FL), Vol. 1, pp. 113–138.
5. Trelstad, R. L. (1982) *Cell* **28**, 197–198.
6. Trelstad, R. L., Birk, D. E. & Silver, F. H. (1982) *J. Invest. Dermatol.* **79**, 109s–112s.
7. Trelstad, R. L. & Birk, D. E. (1984) in *Extracellular Matrix in Development*, ed. Trelstad, R. L. (Liss, New York), pp. 513–543.
8. Trelstad, R. L. & Hayashi, K. (1979) *Dev. Biol.* **71**, 228–242.
9. Birk, D. E. & Trelstad, R. L. (1985) *Ann. N.Y. Acad. Sci.* **460**, 258–266.
10. Birk, D. E. & Trelstad, R. L. (1984) *J. Cell Biol.* **99**, 2024–2033.
11. Birk, D. E. & Trelstad, R. L. (1986) *J. Cell Biol.* **103**, 231–240.
12. Yang, G. C. H. & Birk, D. E. (1988) *J. Ultrastruct. Mol. Struct. Res.* **97**, 238–248.
13. Hamburger, V. & Hamilton, H. L. (1951) *J. Morphol.* **88**, 49–92.
14. Porter, K. R. & Pappas, G. D. (1959) *J. Biophys. Biochem. Cytol.* **5**, 153–166.
15. Haworth, R. A. & Chapman, J. A. (1977) *Biopolymers* **16**, 1897–1906.
16. Holmes, D. F. & Chapman, J. A. (1979) *Biochem. Biophys. Res. Commun.* **87**, 993–999.
17. Stopak, D., Wessels, N. K. & Harris, A. K. (1985) *Proc. Natl. Acad. Sci. USA* **82**, 2804–2808.
18. Harris, A. K., Stopak, D. & Wild, P. (1981) *Nature (London)* **290**, 249–251.
19. Parry, D. A. D. & Craig, A. S. (1988) in *Collagen*, ed. Nimni, M. E. (CRC, Boca Raton, FL), Vol. 2, pp. 1–24.
20. Parry, D. A. D. & Craig, A. S. (1984) in *Ultrastructure of the Connective Tissue Matrix*, eds. Ruggeri, A. & Motta, P. M. (Nijhoff, Boston), pp. 34–64.
21. Eikenberry, E. R., Brodsky, B. & Parry, D. A. D. (1982) *Int. J. Biol. Macromol.* **4**, 322–328.
22. Eikenberry, E. F., Brodsky, B., Craig, A. S. & Parry, D. A. D. (1982) *Int. J. Biol. Macromol.* **4**, 393–398.
23. Scott, J. E. (1984) *Biochem. J.* **252**, 313–323.
24. Krummel, T. M., Nelson, J. M., Diegelmann, R. F., Lindblad, W. J., Salzberg, A. M., Greenfield, L. J. & Cohen, I. K. (1987) *J. Pediatr. Surg.* **22**, 640–644.